PNAS
www.pnas.org

Supplementary Information for

Human impact on the diversity and virulence of the ubiquitous zoonotic parasite *Toxoplasma gondii*

E. Keats Shwab[a, 1], Pooja Saraf[a, 1], Xing-Quan Zhu[b], Dong-Hui Zhou[b], Brent M. McFerrin[c], Daniel Ajzenberg[d], Gereon Schares[e], Kenneth Hammond-Aryee[f], Paul van Helden[f], Steve Higgins[a], Richard W. Gerhold[g], Benjamin M. Rosenthal[h], Xiaopeng Zhao[c,] , Jitender P. Dubey[h,2], Chunlei Su[a,b,2]

Chunlei Su and Jitender P. Dubey
Email: csu1@utk.edu; and jitender.dubey@ars.usda.gov

This PDF file includes:

Supplementary text
Figs. S1 to S4
Tables S1 to S2
References for SI reference citations

Other supplementary materials for this manuscript include the following:

Dataset S1
Dataset S2

www.pnas.org/cgi/doi/10.1073/pnas.1722202115

Supplementary text

Background and supplemental methods for modeling and simulation. The model in this manuscript is a result of a group of researchers' effort on *T. gondii* modeling in the past 8 years. Our adventure on *T. gondii* modeling started at a workshop in 2010 on mathematical modeling of *T. gondii* sponsored by the National Institute for Mathematical and Biological Synthesis (NIMBioS). As one outcome of the workshop, a working group was later supported by NIMBioS to continue the work on *T. gondii* modeling. Below for information on the workshop and working group.

Investigative Workshop on "Mathematical modeling of life cycle, stage conversion, and clonal expansion of Toxoplasma gondii," May 2010. See details of the workshop at the link: http://www.nimbios.org/workshops/WS_Toxoplasma

Working Group on "Integrated Modeling and Analysis of within-host Infection and between-host Transmission for Toxoplasma gondii," May 2011- July 2013. See details of the working group at the link: http://www.nimbios.org/workinggroups/WG_Tgondii

The workshop and the working group have produced a number of publications on *T. gondii* modeling at within-host scale, between-host scale, as well as ecological scale. See publications at the links to the workshop and the working group. The current manuscript is a continuation of the outcome of the workshop and working group. The model used in this work was modified from our previously published agent-based models (ABM) for *T. gondii* transmission dynamics. Both papers were cited in the current manuscript. The papers are attached here for reference. While developing these models, we have conducted extensive literature survey to collect reliable parameters and to describe a detailed life cycle as accurate as possible.

In the 2012 Journal of Theoretical Biology paper (Jiang et al., An agent-based model for the transmission dynamics of *Toxoplasma gondii*. JTB, 2012, 293:15-26), we synthesized what is known about the natural history of *T. gondii* by developing an agent-based model to mimic the transmission process of *T. gondii* in a farm system. The model takes into account the complete life cycle of *T. gondii*, which includes the transitions of the parasite from cats to environment through feces, from contaminated environment to mice through oocysts, from mice to cats through tissue cysts, from environment to cats through oocysts as well as the vertical transmission among mice.

In 2014, we updated the agent-based model (Gotteland et al., Agricultural landscape and spatial distribution of *Toxoplasma gondii* in rural environment: an agent-based model. Int. J. Health Geographics, 2014, 13:45). The improvements in this paper include updates in biological parameters, explicit modeling of dispersion, modeling of landscape, as well as more accurate descriptions of population dynamics and transmission dynamics. In this IJHG paper, we studied how landscape structures impact on the spatial distribution of *T. gondii* prevalence in its rodent intermediate host as well as contamination in the environment. The rural landscape was characterized by the location of farm buildings, which provide shelters and resources for the cats. Specifically, we considered two

configurations of farm buildings, i.e. inside and outside a village. Simulations of the first setting, with farm buildings inside the village, were validated using data from previous field studies. Then, simulation results of the two settings were compared to investigate the influences of the farm locations. We compared 10-year simulation results of the model against field studies in Briquenay, France (field study done by Emmanuelle Gilot-Fromont's group) and the results are consistent.

The purpose of the current manuscript is to investigate the evolutionary outcome of *T. gondii* life cycle in the long run. As part of the manuscript, we will distribute the source code of the model to the public. The current model is implemented using NetLogo, which is well accepted for its broad use in agent-based modeling. We have simulated the model for dozens of times to ensure the long term simulation results are stable and consistent with theory. Prof. Jorge X. Velasco Hernández has independently simulated the model to study the superinfection mechanism in the model. His concluded that the results (of the model) agree with theory: competitive exclusion in the absence of superinfection.

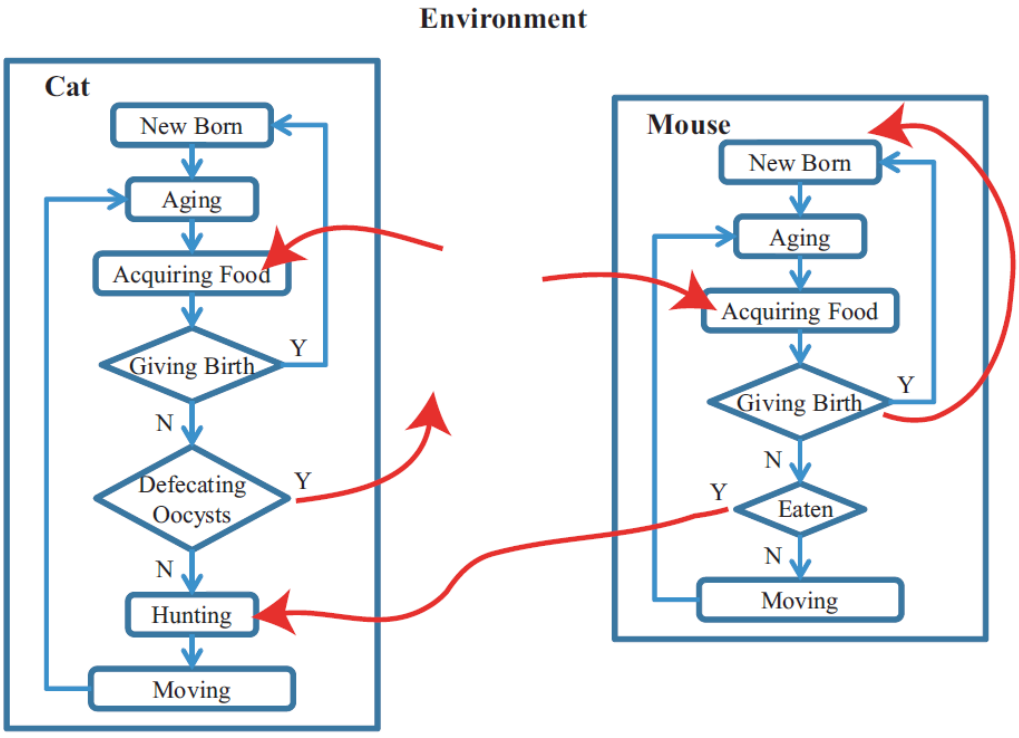

Fig. S1. The components of simulations. Simulated environments consisted of variables including cats, mice, the environment and the parasites. The cats and mice were programmed to move randomly within the area of a spatial patch, interacting when a cat and a mouse occupied the same point on the patch. If the mouse were a carrier of *T. gondii*, the cat would then become infected if consume the mouse. Following infection, cats shed oocysts into the environment, which persisted for a specified period of time. Encounter of oocysts by mice or other cats resulted in those animals becoming infected. If mice were to become infected by *T. gondii*, they would die between 7 and 21 days later with a probability depending on each parasite virulence category. Survivors remained chronic carriers of the parasite for the duration of their lifespan. If a chronically infected mouse were to encounter an oocyst of a different virulence category, the strain would re-infect that mouse with a probability value specified for each virulence category.

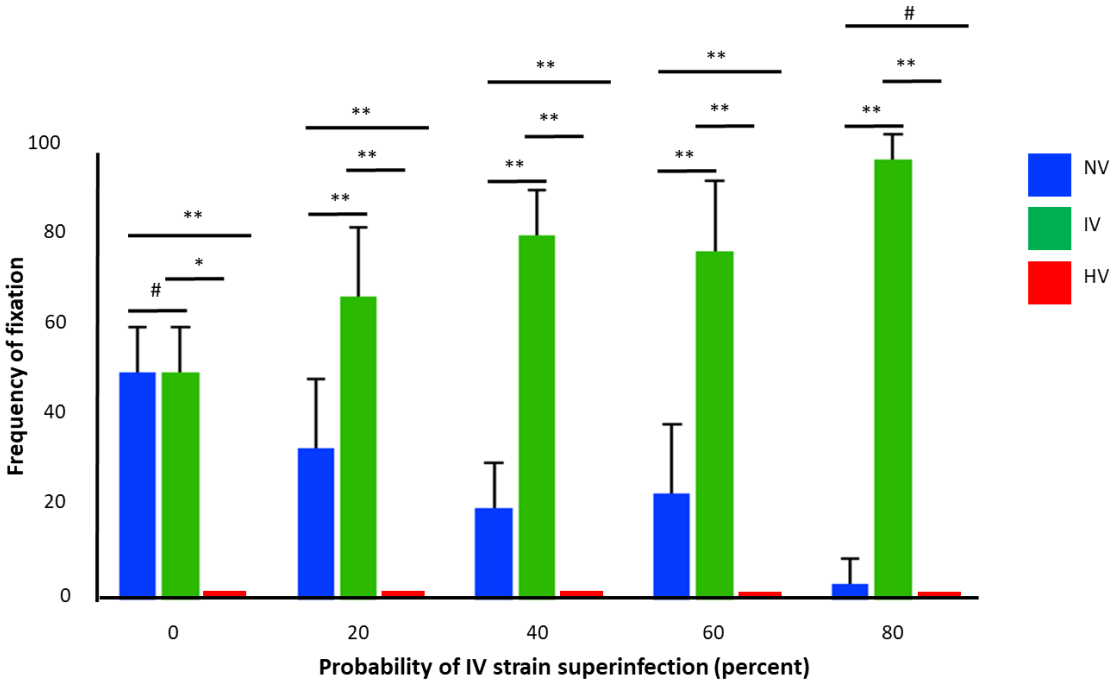

Fig. S2. Increased probability of superinfection by intermediately virulent (IV) strain correlates with increased strain dominance within the domestic cycle. Simulation of changes in population structure as a result of increasing probability of superinfection of mice for IV *T. gondii* was accomplished by running three sets of ten simulations for each of five assigned probabilities of superinfection for this strain type, including probabilities of 0, 20, 40, 60, and 80 percent. All other parameters were kept constant for all simulations and were as follows: Superinfection enabled, vertical transmission disabled, 30 initial cats, 2000 initial mice, 0 initially infected cats, 0 initially infected mice, 6000 initially infected patches, highly virulent (HV) strain mortality rate of 100 percent, IV strain mortality rate of 1 percent, non-virulent (NV) strain mortality rate of 0.1 percent, HV superinfection probability of 100 percent, and NV superinfection probability of 0 percent. Analysis of variance was performed using SAS 9.4 proc glimmix. * $P < 0.01$, ** $P < 0.001$, and # $P > 0.01$.

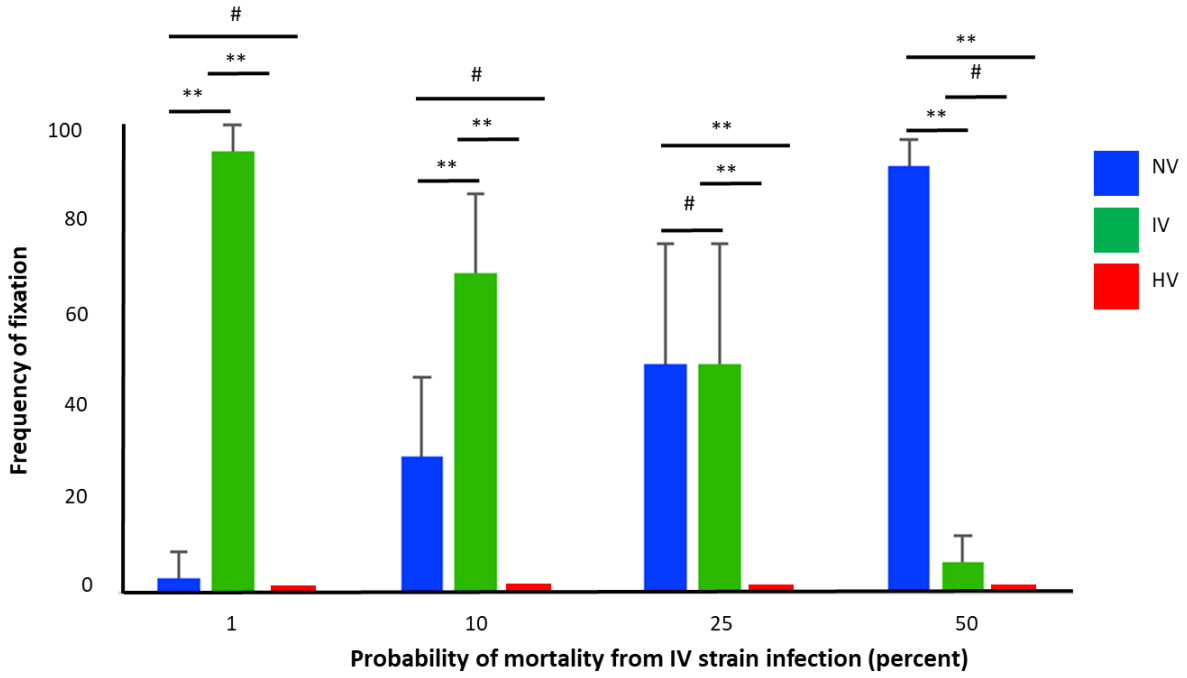

Fig. S3. Increased virulence of IV correlates with its decreased dominance in the domestic cycle. To examine changes in population structure as a result of increasing virulence of the intermediately virulent (IV) train type three sets of ten simulations were run for each of four assigned probabilities of causing mouse mortality for this strain type, including probabilities of 1, 10, 25, and 50 percent. All other parameters were kept constant for all simulations and were as follows: Superinfection and vertical transmission enabled, 30 initial cats, 2000 initial mice, 0 initially infected cats, 0 initially infected mice, 6000 initially infected patches, highly virulent (HV) strain mortality rate of 100 percent, non-virulent (NV) strain mortality rate of 0.1 percent, HV superinfection probability of 100 percent, IV superinfection probability of 80 percent, and NV superinfection probability of 0 percent. Each simulation was run until one strain became fixed in the population after the other two were eliminated from cats, mice and patches. The number of times each strain type became fixed within each of the three sets of ten simulations run for each IV mortality probability was averaged and averages for each strain type were plotted against IV mortality probability. Proportions of IV and NV fixation for each probability were compared and analyzed for statistical differences using SAS 9.4 proc glimmix. Error bars represent standard deviation measurements. * $P < 0.01$, ** $P < 0.001$, and # $P > 0.01$.

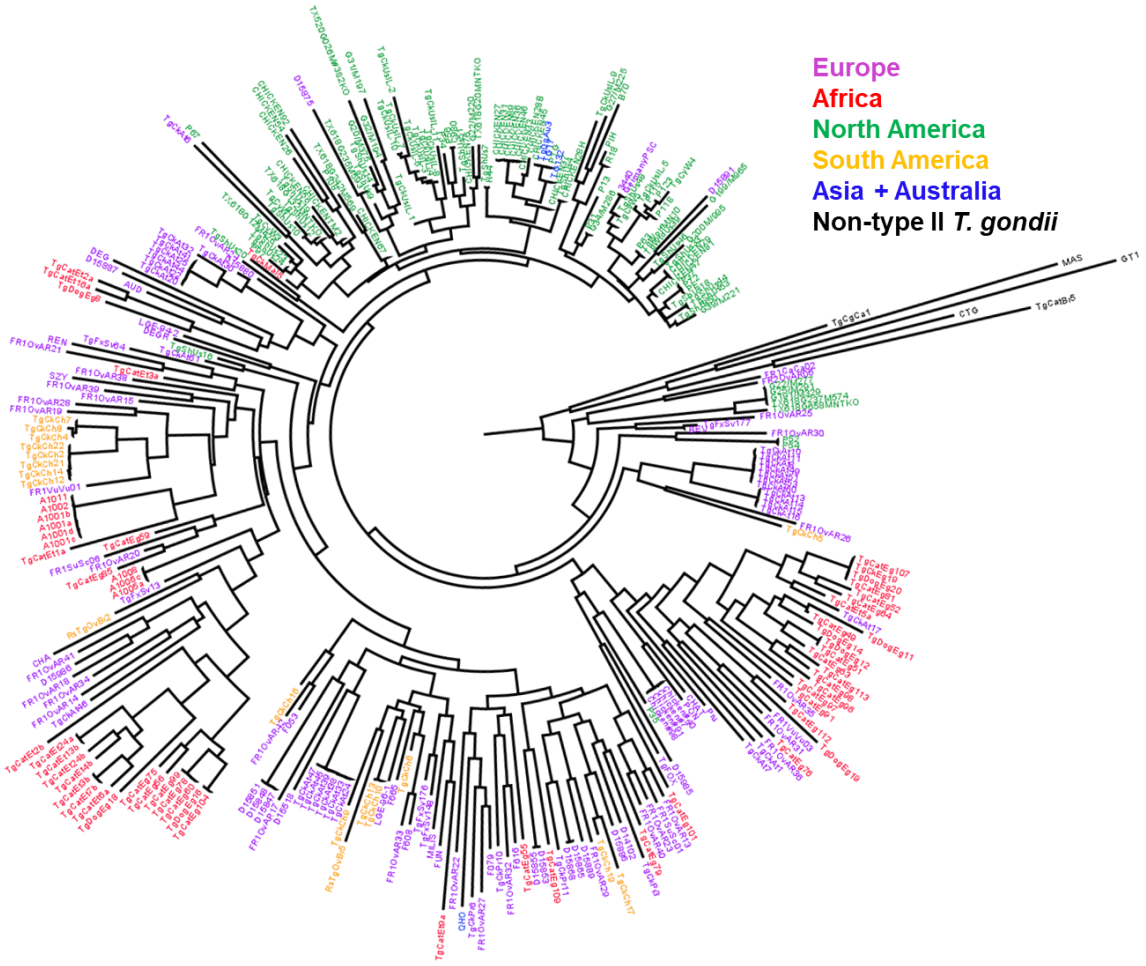

Fig. S4. Rooted Neighbor-joining tree for Type II (ToxoDB PCR-RFLP genotypes #1 and #3) *T. gondii* samples based on 15 microsatellite markers. Non-type II *T. gondii* strains were used as outgroup. Samples from different locations are color-coded.

Table S1. Summary of previous studies relating to *T. gondii* sequential infection of mice

Host line	Inoculation method	Primary infecting strain	Inoculum (cysts)	% Mortality (naive mice)	Secondary infecting strain	Inoculum (cysts)	% Mortality (naive mice)	% Re-infection	Reference
Swiss-Webster	IP	C37	10^5 Tachy	0	RH	10^6 Tachy	ND	≥33	1
NMRI/ Bom	Sub-cutaneous	BEV	Cysts (in-determinate)	20	RH	Cysts (in-determinate)	ND	≥53	2
Swiss-Webster	Oral	ME49	≤500	0	C56	5	100	100	3
Swiss-Webster	Oral	ME49	≤500	0	RC56	5	100	100	3
OF1	Oral	76K	10	0	PRU	10	0	0	4
OF1	Oral	PRU	10	0	NED	10	ND	44	4
BALB/c	Oral	D8	20	0	CH3	20	100	38	5
BALB/c	Oral	D8	20	0	EGS	20	100	88	5
BALB/c	Oral	D8	20	0	CH3	20	100	20	6
BALB/c	Oral	D8	20	0	EGS	20	100	71	6
BALB/c	Oral	ME49	20	0	CH3	20	100	44	6
BALB/c	Oral	ME49	20	0	EGS	20	100	100	6
Callomys callosus	Oral	ME49	20	0	TgChBrUD1	100 Tachy	100	80	7
Callomys callosus	Oral	ME49	20	0	TgChBrUD2	100 Tachy	100	100	7
C57BL/6	IP	CEP	10^5 Tachy	0	CEP	$5x10^4$ Tachy	0	0	8
C57BL/6	IP	CEP	10^5 Tachy	0	CEP (ROP18I)	$5x10^4$ Tachy	100	60	8
C57BL/6	IP	CEP	10^5 Tachy	0	PRU	$5x10^4$ Tachy	0	0	8
C57BL/6	IP	CEP	10^5 Tachy	0	PRU (ROP5I)	$5x10^4$ Tachy	100	60	8
C57BL/6	IP	CEP	10^5 Tachy	0	RH	$5x10^4$ Tachy	100	0	8
C57BL/6	IP	CEP	10^5 Tachy	0	S22	$5x10^4$ Tachy	0	0	8
C57BL/6	IP	CEP	10^5 Tachy	0	S22 (ROP5I, ROP18II)	$5x10^4$ Tachy	100	100	8
C57BL/6	IP	PRU	$2x10^2$ Tachy	0	S22 (ROP5I, ROP18II)	$5x10^4$ Tachy	100	100	8

C57BL/6	IP	CEP	10^5 Tachy	0	S23	$5x10^4$ Tachy	100	40	8
C57BL/6	IP	CEP	10^5 Tachy	0	BOF	$5x10^4$ Tachy	50	0	8
C57BL/6	IP	CEP	10^5 Tachy	0	BOF (ROP5I)	$5x10^4$ Tachy	ND	33	8
C57BL/6	IP	CEP	10^5 Tachy	0	MAS	$5x10^4$ Tachy	100	10	8
C57BL/6	IP	CEP	10^5 Tachy	0	GUY-KOE	$5x10^4$ Tachy	100	100	8
C57BL/6	IP	CEP	10^5 Tachy	0	P89	$5x10^4$ Tachy	76	0	8
C57BL/6	IP	CEP	10^5 Tachy	0	COUGAR	$5x10^4$ Tachy	100	0	8

IP – intraperitoneal injection
Tachy = tachyzoite
ToxoDB genotypes for the *T. gondii* strains listed above:
RH - #10 (Type I)
ME49 - #1 (Type II)
BEV, PRU - #3 (Type II variant)
CEP - #2 (Type III)
BOF – #6 (Type BrI). Most strains in this group are highly virulent to mice, but BOF is non-virulent.
TgChBrUD2 - #6 (Type BrI)
TgChBrUD1 - #11 (Type BrII)
P89 (a.k.a TgPgUs15), D8 - #8 (Type BrIII)
MAS – #17 (Type BrIV)
CH3 - #19
EGS – #229
GUY-KOE – #60
COUGAR (a.k.a. TgCgCa1) -#66
S22, S23 - genetic crosses between ME49 (#1, Type II) and CEP (#2, Type III)
C37, C56, RC56, 76K - unknown

Table S2. Mouse virulence (based on cumulative mortality) of dominant *T. gondii* strains from different geographic regions

ToxoDB PCR-RFLP genotype	Tested strains	Region	Avg. mouse mortality %	Mortality range %	Virulence category	References
#1 (Type II)	ME49, PIH, PE	N. America, Europe, Africa	24	0-40	Intermediate	(9, 10, 11)
#2 (Type III)	CTG, VEG, STRL, C56	N. America, Europe, Africa	3	0-13	Low	(9, 10, 11)
#2 (Type III)	35 strains	Tropical Africa (Gabon)	8.3	0-100	Low	(12)
#3 (Type II)	DEG, PRU	N. America, Europe, Africa	3	0-6	Low	(9, 10, 11, 13)
#4 (Type 12)	B41	N. America	71	71	Intermediate	(9, 10, 14)
#5 (Type 12)	ARI, T61, WTD3	N. America	37	10-80	Intermediate	(9, 10, 11, 14)
#6 (Type BrI)	FOU, TgCatBr2, TgCatBr9	S. America	100	100	High	(9, 10, 11)
#6 (Africa 1)*	11 strains	Tropical Africa (Gabon)	90	0-100	High	(12)
#9 (Chinese 1)	TgCtgy1, TgCtwh3, TgCtwh6	E. Asia	66	24-94	Intermediate	(13)
#9 (Chinese 1)	TgC7, TgPYS, TgGJS	E. Asia	34	29-43	Intermediate	This study

Mouse virulence is calculated based on cumulative mortality with three doses of parasites: 10, 100 and 1000.

* For a given strain, one dose (100, 100-1000 or >1000 parasites) was inoculated to three mice, mortality rate was determined 4 weeks post infection.

References

1. Krahenbuhl JL, Blazkovec AA, & Lysenko MG (1971) The use of tissue culture-grown trophozoites of an avirulent strain of *Toxoplasma gondii* for the immunization of mice and guinea pigs. *J Parasitol* 57:386-390.
2. Reikvam S & Lorentzen-Styr AM (1976) Virulence of different strains of *Toxoplasma gondii* and host response in mice. *Nature* 261:508-509.
3. Araujo F, Slifer T, & Kim S (1997) Chronic infection with *Toxoplasma gondii* does not prevent acute disease or colonization of the brain with tissue cysts following reinfection with different strains of the parasite. *J Parasitol* 83:521-522.
4. Dao A, Fortier B, Soete M, Plenat F, & Dubremetz JF (2001) Successful reinfection of chronically infected mice by a different *Toxoplasma gondii* genotype. *Int J Parasitol* 31:63-65.
5. Brandão GP*, et al.* (2009) Experimental reinfection of BALB/c mice with different recombinant type I/III strains of *Toxoplasma gondii:* involvement of IFN-gamma and IL-10. *Mem Inst Oswaldo Cruz.* 104:241-245.
6. Silva LA, Brandão GP, Pinheiro BV, & Vitor RW (2012) Immunosuppression with cyclophosphamide favors reinfection with recombinant *Toxoplasma gondii* strains. *Parasite* 19:249-257.
7. Franco PS*, et al.* (2015) Calomys callosus chronically infected by *Toxoplasma gondii* clonal type II strain and reinfected by Brazilian strains is not able to prevent vertical transmission. *Front Microbiol* 6:181.
8. Jensen KDC*, et al.* (2015) *Toxoplasma gondii* superinfection and virulence during secondary infection correlate with the exact ROP5/ROP18 allelic combination. *mBio* 6:e02280-02214.
9. Dardé ML, Ajzenberg D, & Su C (2014) Molecular Epidemiology and Population Structure of *Toxoplasma gondii*. *Toxoplasma gondii - The model apicomplexan: Perspectives and Methods*, eds Weiss LM & Kim K (Elsevier Ltd., 525 B Street, Suite 1800, San Diego, CA 92101-4495, USA), 2 Ed.
10. Shwab EK*, et al.* (2014) Geographical patterns of *Toxoplasma gondii* genetic diversity revealed by multilocus PCR-RFLP genotyping. *Parasitol* 141:453-461.
11. Khan A, Taylor S, Ajioka JW, Rosenthal BM, & Sibley LD (2009) Selection at a single locus leads to widespread expansion of *Toxoplasma gondii* lineages that are virulent in mice. *PLoS Genet* 5:e1000404.
12. Mercier A*, et al.* (2010) Additional haplogroups of *Toxoplasma gondii* out of Africa: population structure and mouse-virulence of strains from Gabon. *PLoS Negl Trop Dis* 4:e876.
13. Li M*, et al.* (2014) Phylogeny and virulence divergency analyses of *Toxoplasma gondii* isolates from China. *Parasit Vect* 7:133.
14. Khan A*, et al.* (2011) Genetic analyses of atypical *Toxoplasma gondii* strains reveal a fourth clonal lineage in North America. *Int J Parasitol* 41:645-655.

Other supplementary materials (separate file)

Dataset S1. Microsatellite typing results

Dataset S2. Simulation code